A Statistical Model of Right Ventricle in Tetralogy of Fallot for Prediction of Remodelling and Therapy Planning

Abstract. Tetralogy of Fallot (ToF) is a severe congenital heart disease that mainly affects the right ventricle (RV). It requires surgical repair early in infancy. Chronic regurgitations may appear due to damaged pulmonary valves, resulting in extreme RV dilation. To reduce risk factors late after repair, new pulmonary valves must be re-implanted. However, establishing the best timing for re-intervention is a clinical challenge because of the large variability in RV shape and in pathology evolution. The purpose of this study is to quantify the regional impacts of growth and regurgitations on the end-diastolic RV anatomy. The ultimate goal is to determine, among clinical variables, predictors for the shape in order to build a statistical model that predicts RV remodelling. The proposed approach relies on a *forward* model based on currents and LDDMM algorithm to estimate an unbiased template of 18 patients and the deformations towards each individual shape. Then, cross-sectional multivariate analyses are employed to assess the effects of body surface area, tricuspid and transpulmonary valve regurgitations upon the RV shape. The significant deformation modes were found clinically relevant. Canonical correlation analysis was applied to derive a generative model of RV remodelling, which was successfully tested on two new patients.

1 Introduction

Tetralogy of Fallot is a severe congenital heart defect that requires surgical repair early in infancy. Yet, pulmonary valves may be damaged by the surgery, causing chronic regurgitations. As a result, the right ventricle (RV) dilates extremely, its shape is altered and the cardiac function is impaired: new valves must be implanted in adulthood to reduce the risk factors late after repair [1]. Understanding and quantifying RV remodelling in repaired Tetralogy of Fallot (ToF) patients is crucial for patient management and therapy planning. However, the high variability in pathology course and in RV anatomy make difficult the decision of optimal timing for re-intervention [1].

Contrary to the left ventricle, whose shape and deformations under pathological conditions are well documented, RV anatomy is complex and can vary tremendously among ToF patients. Several studies have been published about possible correlations between clinical parameters in ToF [1]. However, few works have quantified the anatomical alterations of the RV and their evolution due to the disease [2, 3]. In [2], the authors measure the most striking differences in RV shape with respect to normals, quantifying the complex RV remodelling

observed in ToF. However, only one-dimensional indices are considered despite the availability of 3D segmentations. In [3], the authors present a 4D Active Appearance Model of the beating heart to segment RV in MRI. They propose indices based on the shape modes and successfully classify patients from normal. Yet, they do not correlate their model with functional features of ToF.

The clinical challenges about ToF encourage applying image-based shape analysis techniques to model the RV anatomical alterations due to pathological factors. These techniques generate a representative template of the population of interest and assess how it deforms within this population [4–7]. Yet, correlating shape with clinical variables require a rigorous framework: Biases may appear if the template is not defined in a consistent way, which may yield drastic differences in the statistical conclusions. Two strategies are available to create the template. The *backward* approach consists in modelling the template as the average of the deformed observations plus some residuals [4, 5]. Such a template can be computed efficiently but the model parameters, especially the residuals, are more difficult to identify. The *forward* approach consists in modelling the observations as deformations of the template plus some residuals [6, 7]. Computing the template is more complex but model parameters can be faithfully estimated from images and clinical data.

In view of assisting the cardiologists in establishing the best time for re-intervention, we aim at statistically predict the RV remodelling in ToF. As a first step, we propose in this work to quantify the regional impacts of growth and regurgitations on the end-diastolic RV anatomy in a cohort of 18 ToF patients. We rely on a *forward* approach to estimate the main deformation modes. Then, cross-sectional multivariate analyses are employed to assess the effects of growth and regurgitations upon the RV shape. This yields a generative model of RV remodelling, model that is then tested on two new patients.

2 Methods

The segmentation of the Right Ventricle (RV) of multiple patients from cine-MRI is described in Sec. 3.1. To perform the analysis on this population of shapes, an unbiased template is first built. This template serves as the reference atlas to determine the deformations towards each individual shape, deformations that are then analysed using a Principal Component Analysis (PCA) to extract the main deformations modes. The importance of each mode is statistically assessed with respect to child growth and valvar regurgitation severity. In particular, we investigate how our generative model can predict the evolution of shape with respect to body surface area.

2.1 Unbiased Template of the Right Ventricle in Tetralogy of Fallot

We apply the *forward* strategy proposed by [7] to generate the RV template. This approach is particularly suited for our purposes as 1) it is non-parametric, shapes being represented by currents; 2) model parameters are well-defined and can be

estimated from clinical data, thus enabling statistical analyses; 3) template and deformations are computed simultaneously and consistently and 4) new patients can be integrated in the study seamlessly, re-estimating the template is not required. More precisely, in the *forward* framework, the RV surfaces, or shapes, are modelled as the sum of a diffeomorphic deformation ϕ^i of the template $\overline{\mathcal{T}}$ and a residual term ϵ^i that models the shape features that cannot be represented by the template (topology changes, acquisition artifacts, etc.): $\mathcal{T}^i = \phi^i.\overline{\mathcal{T}} + \epsilon^i$.

Currents are used to represent the shapes, the residuals and the deformations in the same common framework. Currents form a vector space, thus enabling the usual operations (mean, variance...) on shapes. Intuitively, they can be seen as the flux of any vector field $\omega \in W$ across the shapes. W is a vector space of infinite dimension (a reproducible kernel Hilbert space or RKHS) generated by a Gaussian kernel $K_W(\mathbf{x},\mathbf{y}) = \exp(-\|\mathbf{x}-\mathbf{y}\|^2/\lambda_W^2)$, which defines an inner product in W that can be easily computed. In this framework, a triangle centred at $\mathbf{x}$ with normal α is represented by the Dirac delta current $\delta_{\mathbf{x}}^{\alpha}$. Thus, a discrete mesh is encoded by the sum of the currents of its triangles $\mathcal{T}^i = \sum_k \delta_{\mathbf{x}_k^i}^{\alpha_k^i}$. In such a model, the residuals ϵ^i are naturally modelled as a Gaussian distribution on the α_k^i. The deformation ϕ^i registering the template $\overline{\mathcal{T}}$ to the current $\mathcal{T}^i$ is estimated using the Large Deformation Diffeomorphic Mappings (LDDMM) framework [8]. The key feature is that this deformation can be parametrised by its smooth initial vector speed $\mathbf{v}_0^i$, which also belongs to a Gaussian RKHS with variance λ_V^2. Moreover, this initial speed vector field is completely defined by the *moment* vectors β^i centred at the same point location as the template moments: $\mathbf{v}_0^i(\mathbf{x}) = \sum_k K_V(\mathbf{x}_k,\mathbf{x})\beta_0^i[k]$. A two-step strategy is employed to estimate alternatively the template $\overline{\mathcal{T}}$ and the deformations ϕ^i towards each patient, until convergence. The algorithm is initialised from the mean current of the population.

2.2 Characterising Deformation Modes of RV Shapes in ToF

To assess the shape variabilities we consider the deformations ϕ^i only as we are focused on the regional alterations of the RV anatomy due to ToF. Principal Component Analysis (PCA) is performed directly on the moments β_i to extract the main deformation modes. The elements of the covariance matrix Σ are given by $\Sigma_{ij} = \sum_{\mathbf{x}_k,\mathbf{x}_l}(\beta^i(\mathbf{x}_k) - \overline{\beta}(\mathbf{x}_k))K_V(\mathbf{x}_k,\mathbf{x}_l)(\beta^j(\mathbf{x}_l) - \overline{\beta}(\mathbf{x}_l)) =< \mathbf{v}_0^i - \overline{v_0}, \mathbf{v}_0^j - \overline{v_0} >_V$, $\mathbf{x}_k$ being the positions of the k^{th} Dirac delta currents of $\overline{\mathcal{T}}$. Then, the moment vector γ^m of the initial speed vector $\mathbf{u}_0^m$ that is related to the m^{th} deformation mode is obtained through the reconstruction formula $\gamma^m = \overline{\beta} + \sum_i \mathbf{V}^m[i](\beta^i - \overline{\beta})$, where $\mathbf{V}_m$ is the m^{th} eigenvector of Σ when the eigenvalues are sorted in decreasing order. Finally, if the M first deformation modes are considered, the RV shape of each patient i is characterised by the shape vector $\mathbf{s}^i$ defined by:

$$\mathbf{s}^i = \{s_m^i\}_{m=1..M} \quad s_m =< \mathbf{v}_0^i, \mathbf{u}_0^m >_V = \sum_{\mathbf{x}_k,\mathbf{x}_l} \beta^i(\mathbf{x}_k)K_V(\mathbf{x}_k,\mathbf{x}_l)\gamma^m(\mathbf{x}_l) \qquad (1)$$

2.3 Can We Predict the Shape from Clinical Parameters?

First, cross-sectional analysis of the impact of growth on RV shape was performed. Multiple linear regression between the shape vectors $\mathbf{s}^i$ and body surface area (BSA) was carried out to exhibit the effects of BSA on each deformation mode. To refine the model, non-related deformation modes were removed using step-wise variable reduction until the overall significance of the regression stopped decreasing, thus yielding an optimal set of deformation modes. Canonical Correlation Analysis (CCA) was then applied to quantify the amount of variation of each deformation mode when BSA varies. If R is the overall correlation coefficient between BSA and shape vectors, and ρ is the correlation vector relating each deformation mode with BSA, then the moments μ of the generative deformation Φ are $\mu = R \sum_k \rho[k]\gamma^k$. Deforming the template $\overline{\mathcal{T}}$ with Φ enables quantifying the average RV remodelling observed in our population.

Second, we assessed the impact of tricuspid and transpulmonary regurgitations on each deformation mode. Two independent analyses were carried out because of the small number of subjects (18). As regurgitations were quantified through a five-level index, rank-based Kruskal-Wallis analysis of variance was applied. If an effect was found for some deformation modes, post-hoc two-sample rank-based Wilconxon tests were used to determine which levels differed.

All the statistical tests were carried out using the shape vectors $\mathbf{s}^i$ (Equation 1). The level of significance was set at $p < 0.1$ and multiple comparisons were corrected using Bonferroni adjustment.

3 Experiments and Results

3.1 Data Collection

Subjects and Image Preparation We selected 18 patients (8 males, mean age $\pm$ SD $= 15 \pm 3$) with repaired Tetralogy of Fallot (ToF). Body-surface area (BSA) was reported for each patient (Dubois formula, mean $\pm$ SD $= 1.53 \pm 0.3$). Steady-State Free Precession cine MRI of the heart were acquired during a single breath-hold with a 1.5T MR scanner (Avanto, Siemens). Images were acquired in the short-axis view covering entirely both ventricles (10-15 slices; isotropic in-plane resolution: 1.1x1.1mm to 1.7x1.7mm; slice thickness: 6-10mm; temporal resolution: 25-40 phases). Tricubic resampling was performed to obtain isotropic voxel sizes defined by the in-plane resolution.

Surface Meshes Preparation End-diastolic RV endocardium was segmented on the MRI cardiac sequence by fitting an anatomically accurate geometrical model. Its position, orientation and scale in the image was determined using minimal user interaction. Then, local boundaries were estimated by training a probabilistic boosting tree classifier with steerable features [9]. To reduce positioning effects in the shape analysis, the RV meshes were rigidly registered to a representative patient of the dataset by using GMMReg[1] [10]. The results were visually inspected and remaining undesirable rotations were corrected manually (Fig. 1, left panel).

[1] http://code.google.com/p/gmmreg/

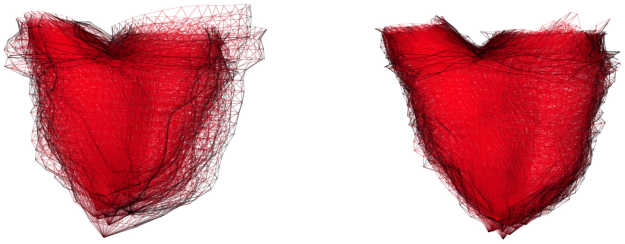

Rigid alignment Non-linear registration to the template

Fig. 1. 3D RV mesh of 18 ToF patients. *Left panel:* The meshes were rigidly registered to a representative patient of the dataset. Observe the extreme variability in shape *(see companion video). Right panel:* The same meshes registered to the template using the non-linear deformations estimated during the template creation.

3.2 Statistical Shape Model of the Right Ventricles

Building the template $\overline{\mathcal{T}}$ required setting two parameters (Sec. 2): λ_V, which defines the "stiffness" of the non-linear deformations (the higher is λ_V, the more global is the transformation); and λ_W, which characterises the resolution of the currents representation (low λ_W values enable analysing subtle shape features). As we were mainly interested in the regional ToF alterations (dilation, valve enlargement, regional bulging), these parameters were set to $\lambda_W = \lambda_V = 15$mm, about the diameter of the RV outflow tract. Lower values would have been inappropriate as the slice thickness of the images was approximately 10mm.

One iteration of the alternate minimisation was needed to reach convergence. Yet, the resulting template $\overline{\mathcal{T}}$ was well centred (mean over standard deviation of the deformations was 0.8). The first 10 deformation modes were selected, representing more than 90% of the total energy (Fig. 2).

The most similar patient to the template provided interesting insights about the "fictitious" clinical setting that would have had the RV template. The age of this patient was 17 and his BSA 1.76, both indices being close to the observed mean. This suggest that in our population, the mean shape corresponded also to the mean BSA and age. More interestingly, this patient had trace valvar regurgitations only, which is not surprising when considering the shape of the template: no striking pathological bulging were visible.

3.3 Statistical Model of RV Remodelling in ToF Patient

Patient growth was quantified by body surface area (BSA) index (correlation with age in the data set: $R^2 > 0.5, p < 0.001$). Multiple linear regression between BSA and shape vectors $\mathbf{s}$ (Sec. 2.2) writes as: $\text{BSA} = a_0 + \sum_{l=1}^{10} a_l \mathbf{s}[l]$. Table 1 reports the regression coefficients a_l, the related t-values and the overall model significance ($R^2 > 0.8, p < 0.05$). The sign of the a_l relates to the direction of the deformation modes (negative a_l meaning backwards deformations). After model reduction, only the six deformation modes that were found significant remained ($R^2 > 0.7, p < 0.01$) (Table 1). Visual inspection of the modes with an

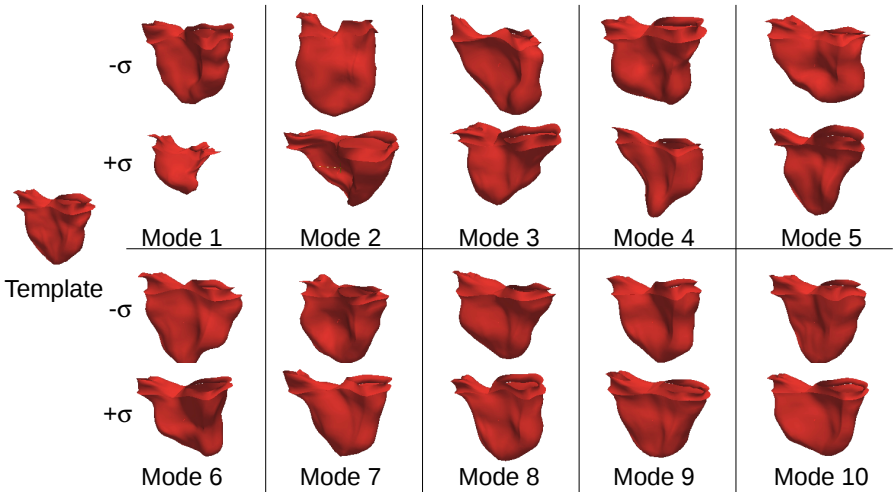

Fig. 2. 10 first deformation modes extracted by PCA a population of 18 patients suffering from repaired Tetralogy of Fallot.

expert demonstrated their clinical relevance (Fig. 2). Mode 1 clearly represented the overall RV dilation. Mode 2 seemed to model the dilation of the tricuspid annulus and of the inflow tract. Mode 3, 6, 7 and 9 exhibited a dilation of a specific RV region: apex (mode 3), basal area under the tricuspid valve (mode 6), apical area of the outflow tract (mode 7) and outflow tract (mode 9), reflecting possible direct impact of regurgitations on the neighbouring tissues.

Canonical Correlation Analysis (CCA) was performed to obtain a generative model of the RV remodelling observed in our population. Overall correlation coefficient with BSA was $R = 0.87$, suggesting a strong correlation between these deformation modes and child growth. The correlation vector related to the deformation modes was $\rho = \{-0.56, 0.45, -0.35, -0.33, -0.33, -0.37\}$. When BSA increased by 0.86, each deformation mode m varied according to its related coefficient $\rho[m]$. The model was found clinically relevant by an expert (Fig. 3). As BSA increased, RV volume increased, RV free-wall and valves dilated, and

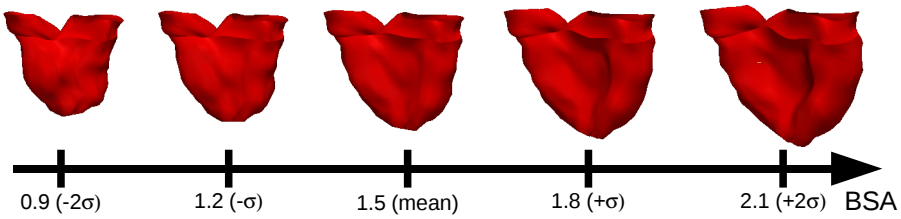

Fig. 3. Mean RV remodelling observed in our population when body surface area (BSA) increases (BSA in m^2). We can observe a global increase of RV dimensions and dilation of the valves. Simultaneously, RV free wall becomes rounder and septum more concave (see companion videos).

septum was more concave. This is clinically meaningful since, as the valves dilates, remaining pulmonary obstructions disappear, thus decreasing the right ventricular pressure. As a result, left-ventricle pushes the septum inwards the right ventricle, making it more concave. Yet, as regurgitations are still present, the RV still dilates by pushing the RV freewall outwards.

3.4 Quantifying the Impact of Valvar Regurgitations on RV Shape

Colour Doppler ultrasound (sweep speeds: 50-100 mm/s) was used to quantify tricuspid (TriReg) and transpulmonary valve (TPVReg) regurgitations. To assess the effects of TPVReg, patients were grouped into two different groups: trace TPVReg and severe TPVReg. Kruskal-Wallis analysis revealed a significant effect on deformation mode 2 ($p < 0.1$), which was confirmed by visual inspection (Fig. 2) as this mode exhibited an elongation of the RV outflow tract.

Evaluation of TriReg classified the patients into 3 groups: none, trace or mild tricuspid regurgitations. Kruskal-Wallis analysis showed a significant impact of TriReg on three deformation modes: 3 ($p < 0.05$), 6 ($p < 0.1$) and 8 ($p < 0.1$). However, pair-wise Wilconxon tests showed that only mode 3 had two significant different levels (trace TriReg versus mild TriReg, $p < 0.1$). Visually, deformation mode 3 exhibited a striking deformation of the tricuspid annulus, from circular to triangular-shape, and a dilation of the RV inflow tract.

It is worth observing that two deformation modes involved in the statistical model of RV growth were also related to the regurgitation severity. This may suggest possible cross-effects between growth and regurgitations on these specific shape variations.

3.5 Validating the Generalisation of the Statistical Models

Generalising a statistical model of RV remodelling is of primary importance for patient management and therapy planning. Thus, the robustness of our statistical model of RV remodelling (Sec. 3.3) was tested on two new patients with matched age (13 and 16). The template was registered to the patients and the related shape vectors $\mathbf{s}^{1,2}$ were computed. BSA were estimated from the 6-mode linear model (Sec. 3.3). Results were successfully compared to measured values (patient 1: estimated BSA = 1.61, measured BSA = 1.49; patient 2: estimated BSA: 1.29, measured BSA: 1.16). This suggests that the deformation modes

Table 1. Linear regression coefficients a_l between shape modes and BSA. In bold the significant coefficients ($p < 0.1$). After model reduction (second array), coefficients stay unchanged, confirming the stability of the statistical test.

	Overall Significance	$\mathbf{a_1}$	a_2	a_3	a_4	a_5	a_6	a_7	a_8	a_9	a_{10}
Coef. $\times 10^{-5}$	$R^2 = 0.84, p = 0.04$	**-2.9**	**6.4**	**-7.6**	4.6	-1.0	**-11.1**	**-11.9**	7.0	**-20.1**	-15.4
t-values		-3.28	2.64	-2.04	1.13	-0.19	-1.93	-1.92	0.84	-2.15	-1.43
Coef. $\times 10^{-5}$	$R^2 = 0.75, p = 0.006$	**-2.9**	**6.4**	**-7.6**			**-11.1**	**-11.9**		**-20.0**	
t-values		-3.27	2.63	-2.03			-1.92	-1.92		-2.14	

involved in the linear model of RV remodelling could be generalised, thus constituting potential quantitative parameters of RV remodelling in ToF.

4 Discussion and Future Works

In this study we investigated the impact of child growth and valvar regurgitations on RV anatomy at end diastole in patients suffering from repaired ToF. End-diastolic time point was chosen as it is the time when the effects of the pathology are the most evident [1, 2]. From multivariate statistical analyses, we derived a generative model of the observed RV remodelling. This model, as well as the deformation modes that were found significantly related to growth and regurgitations, were clinically relevant as they exhibited realistic alterations in RV anatomy. Incorporating more patients is now required to confirm these findings. Adding more patients would enable identifying different groups of RV remodelling (with aneurysm, with stiff myocardium, etc.), which might be of crucial interest when deciding for valve replacement. Future works also include analysing the 4D cardiac motion. To the best of our knowledge, this study constitutes a first attempt in correlating 3D shape parameters to clinical measurements in ToF. These analyses may yield quantitative image-based predictors about RV anatomy and remodelling in ToF.

References

1. Geva, T.: Indications and timing of pulmonary valve replacement after tetralogy of Fallot repair. In: Sem. Thor. and Card. Surg.: Ped. Card. Surg. Annual. Volume 9., (2006) 11–22
2. Sheehan, F., Ge, S., Vick III, G., Urnes, K., Kerwin, W., Bolson, E., Chung, T., Kovalchin, J., Sahn, D., Jerosch-Herold, M., et al.: Three-Dimensional Shape Analysis of Right Ventricular Remodeling in Repaired Tetralogy of Fallot. The American Journal of Cardiology (2007)
3. Zhang, H., Walker, N., Mitchell, S., Thomas, M., Wahle, A., Scholz, T., Sonka, M.: Analysis of four-dimensional cardiac ventricular magnetic resonance images using statistical models of ventricular shape and cardiac motion. In: Proc. SPIE 2006.
4. Guimond, A., Meunier, J., Thirion, J.P.: Average brain models: A convergence study. Computer Vision and Image Understanding **77**(2) (2000) 192–210
5. Joshi, S., Davis, B., Jomier, M., Gerig, G.: Unbiased diffeomorphic atlas construction for computational anatomy. NeuroImage **23** (2004) 151–160
6. Allassonniere, S., Amit, Y., Trouve, A.: Towards a coherent statistical framework for dense deformable template estimation. Journal of the Royal Statistical Society: Series B (Statistical Methodology) **69**(1) (2007) 3–29
7. Durrleman, S., Pennec, X., Trouvé, A., Ayache, N.: A forward model to build unbiased atlases from curves and surfaces. In: Proc. MFCA 2008.
8. Vaillant, M., Glaunes, J.: Surface matching via currents. In: Proc. IPMI 2005. 381
9. Zheng, Y., Barbu, A., Georgescu, B., Scheuering, M., Comaniciu, D.: Fast automatic heart chamber segmentation from 3D CT data using marginal space learning and steerable features. In: Proc. ICCV 2007. 1–8
10. Jian, B., Vemuri, B.: A robust algorithm for point set registration using mixture of Gaussians. In: Proc. ICCV 2005. 1246–1251